Ghost Plumes: Artificial splitting of greenhouse gas emission plumes in passive remote sensing observations in special viewing geometries

S. Krautwurst[1], J. Borchardt[1], Sebastian Wolff[2], O. Huhs[1], K. Gerilowski[1] , Christian Fruck[2], Christoph Kiemle[2], Mathieu Quatrevalet[2], Martin Wirth, J. P. Burrows[1], A. Fix[2], H. Boesch[1], H. Bovensmann[1] and the CoMet 2.0 Arctic Team

[1]Institute of Environmental Physics (IUP), University of Bremen, Bremen, Germany

[2]Deutsches Zentrum für Luft- und Raumfahrt (DLR), Institut für Physik der Atmosphäre, Oberpfaffenhofen, Germany

Objectives & experimental approach

Scientific goals address the following questions:

- How are emission plumes actually "seen" (i.e. identified) by active and **passive remote sensing** instruments (airborne and satellite) in a simplified world (ignoring atmospheric turbulence)?
- What are the possible **implications** for the retrieval algorithms of flux estimates?

Experimental setup (during CoMet 2.0 Arctic 2022, HALO): [Krautwurst, 2024]

- **Passive airborne remote sensing by the imaging spectrometer MAMAP2D-Light (M2DL)**
- Active airborne remote sensing by the greenhouse gas Lidar **CHARM-F**
- Both are mounted on the **same platform** (**HALO @ ~8 km flight altitude**) probing atmospheric CH_4 and CO_2 concentrations (column observations)

The MAMAP2D-Light imager (passive) & the CHARM-F GHG Lidar (active)

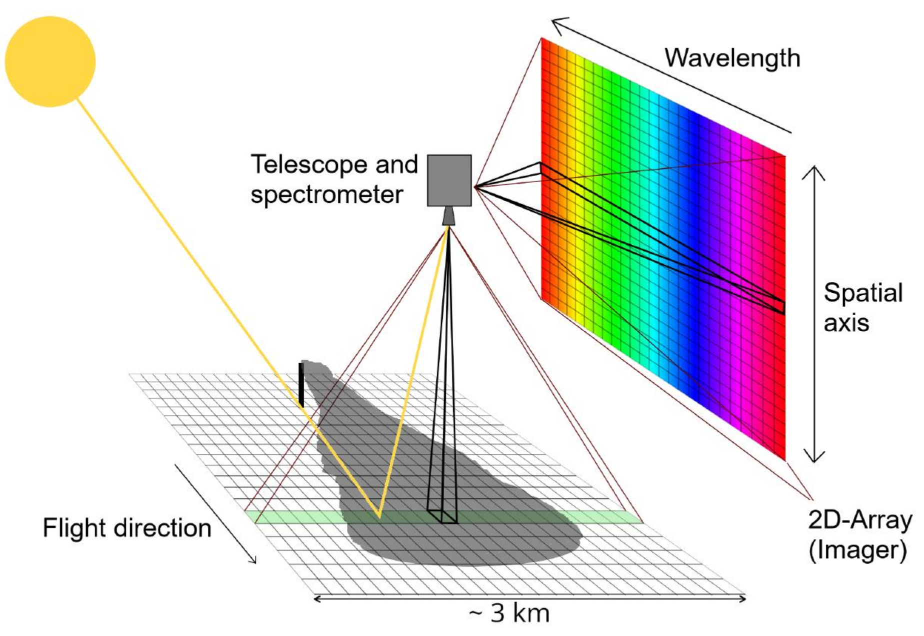

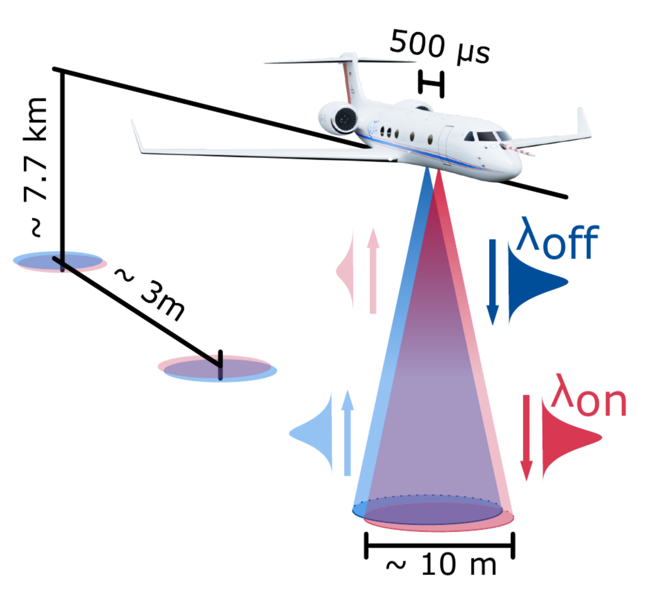

Fig. 1: Measurement geometries. *Left:* Schematic of the MAMAP2D-Light push broom spectrometer with a ground scene size of about 110 m in the traverse direction of flight at a flight altitude of around 8 km a.g.l. *Right:* Schematic of the CHARM-F GHG Lidar system.

Theory: Actually integrated light path in line of sight for passive and active remote sensing

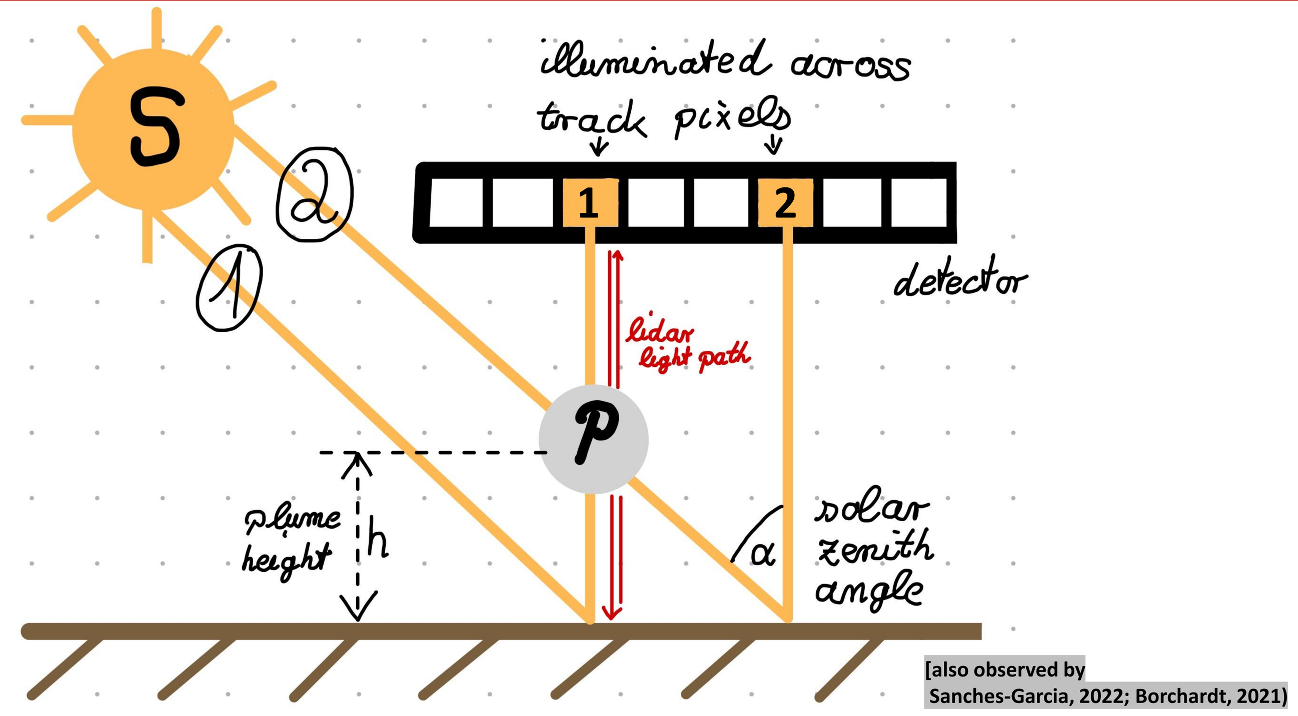

Fig. 2: The schematic shows an idealised confined plume (P) moving into the screen overflown by an aircraft carrying a passive remote sensing instrument (flying also into the screen). Two idealised solar rays are also shown. The (1) is first reflected from the ground and then passes through the plume, and the (2) first passes through the plume before being reflected and then detected by the detector of the instrument. Although both rays cross the same plume, they result in two different plume signals on the detector. Red arrows indicate the light from a lidar crossing the plume only vertically.

Ghost Plumes: Simulations (of passive RS) vs. Observations (of passive and active RS)

1) Gaussian 3D Plume model simulations (incl. plume rise) [Krings, 2011; Masters, 1998, Hanna, 1982]

$$C(x,y,z) = \frac{F}{\pi \sigma_y(x) \sigma_z(x) u} \exp\left(-\frac{1}{2}\left(\frac{y}{\sigma_y(x)}\right)^2\right) \exp\left(-\frac{1}{2}\left(\frac{z}{\sigma_z(x)}\right)^2\right)$$

Eq. 1: Quasi-stationary Gaussian plume model.

Fig. 3 (bottom and right): Plume simulation based on different parameterizations. Standard scenario:

solar azimuth angle: 225° (SW) | stack height: 130 m
solar zenith angle: 45° | atmos. stability: slightly unstable
wind speed: 6 m/s | wind direction: south-east (SE)
emission rate: 8.694 Mt CO_2 / yr

The real power plant stack is located at [0,0] and marked by a black cross, and the angle from which the solar radiation is coming is indicated by a yellow disc. The position and shape of the ghost plume depends on input parameters. Bending of the ghost plume is due to the considered plume rise.

a) Different solar azimuth angles (saa)

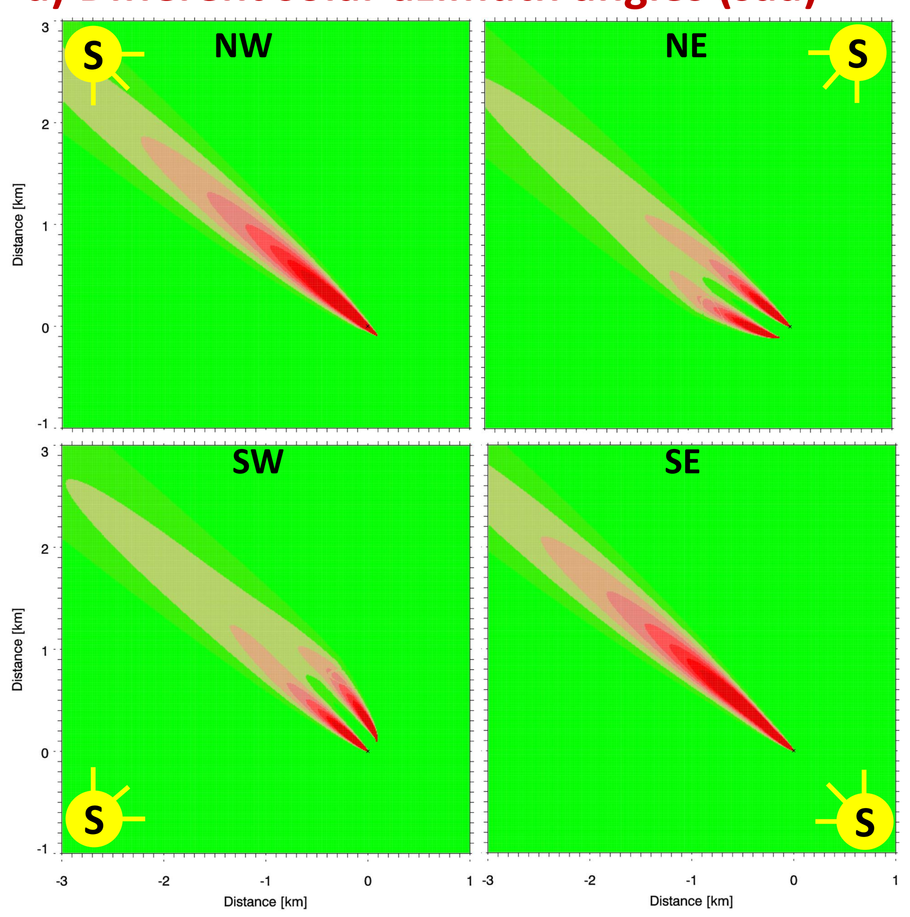

b) Different stack and plume heights

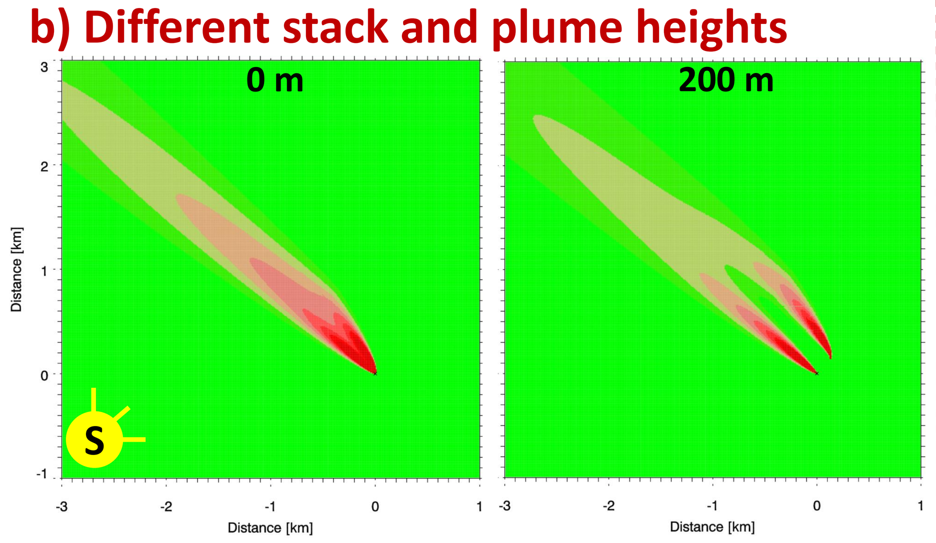

c) Different solar zenith angles (sza)

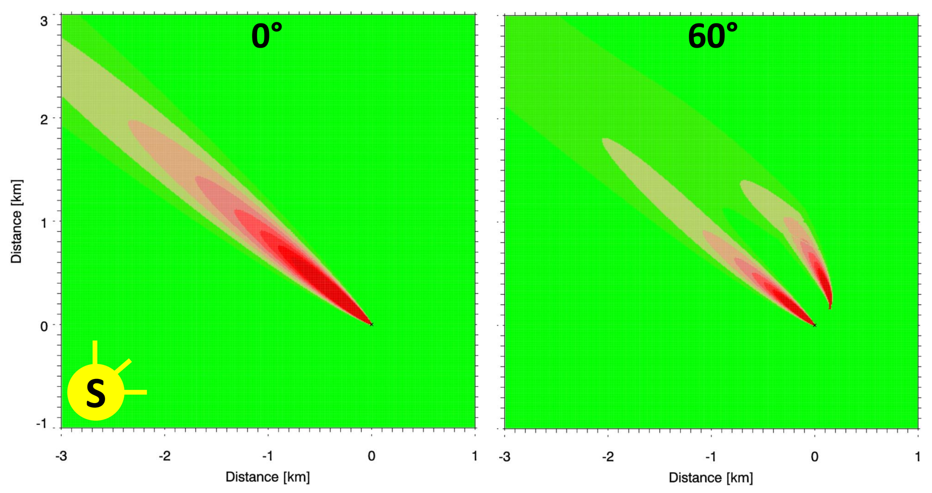

d) Atmospheric stability (class)

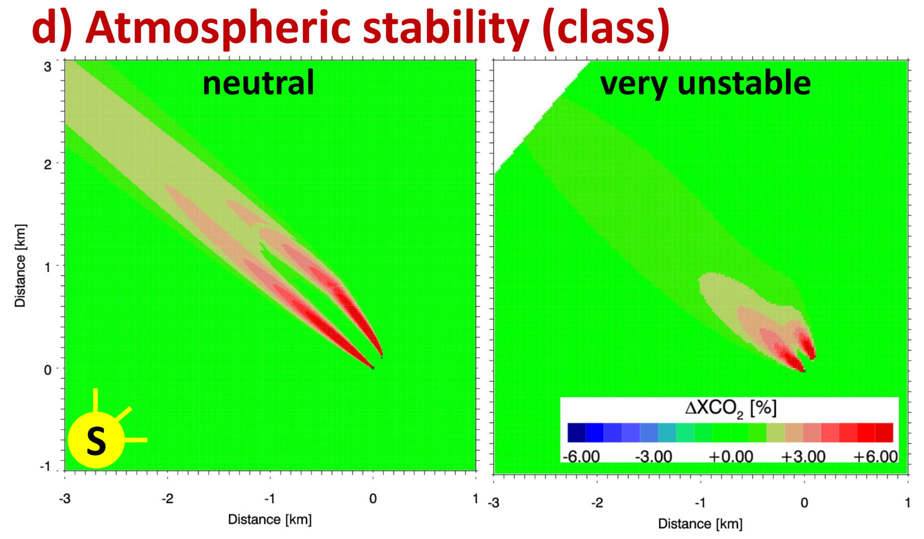

2) MAMAP2D-Light passive RS observations (CO_2 from Power Plant)

Fig. 4: Top: Google Earth imagery of the power plant investigated. The star marks the emission stack. *Bottom right:* Plume simulation adapted to the observation conditions corresponding to the standard scenario from *Fig. 3* (saa: 225° (SW), sza: 45°, height: 130 m, wind: 6 m/s from SE , slightly unstable, 8.7 Mt CO_2 / yr). The distance between the starting points of the two plumes is about 160 m. *Bottom left:* Simulation gridded to simulate different ground scene sizes of an imager.

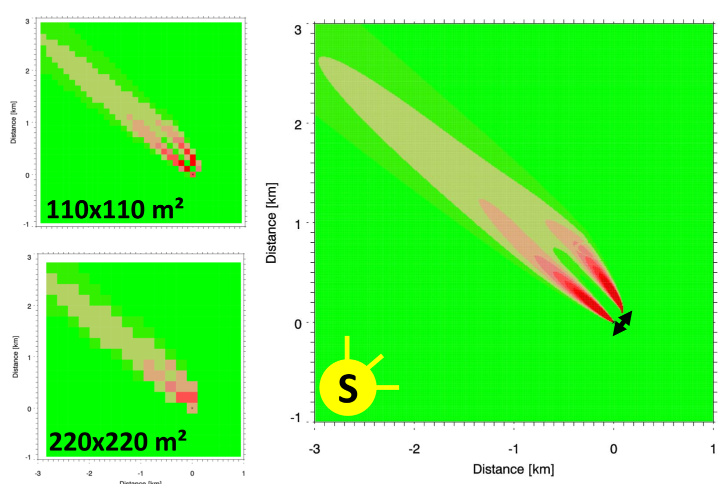

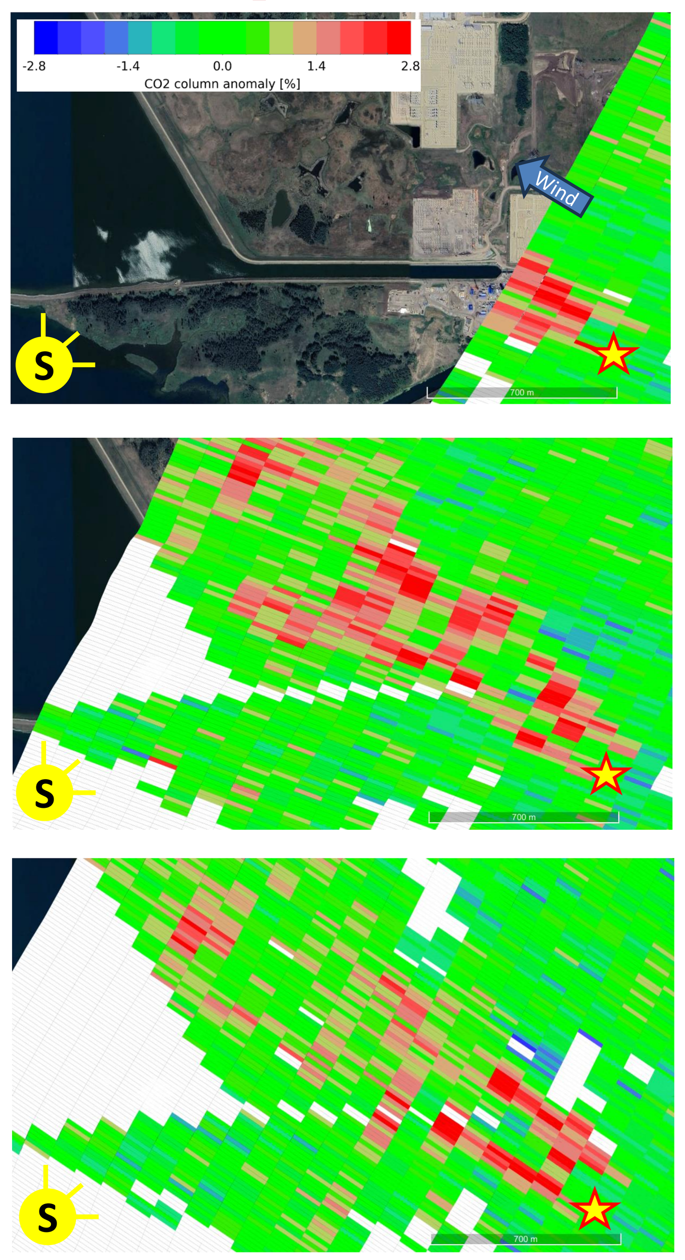

Fig. 5: Three different overflights of the power plant are shown - CO_2 column anomalies retrieved from M2DL data. The star marks the emission stack. All show a distinct ghost plume in the near-field in accordance with the position of the sun. The ground scene size of the M2DL instrument is about 110 m X 8.5 m (across X along track). Measurement geometry matches standard scenario in *Fig. 4, bottom*.

3) Passive vs. active remote sensing

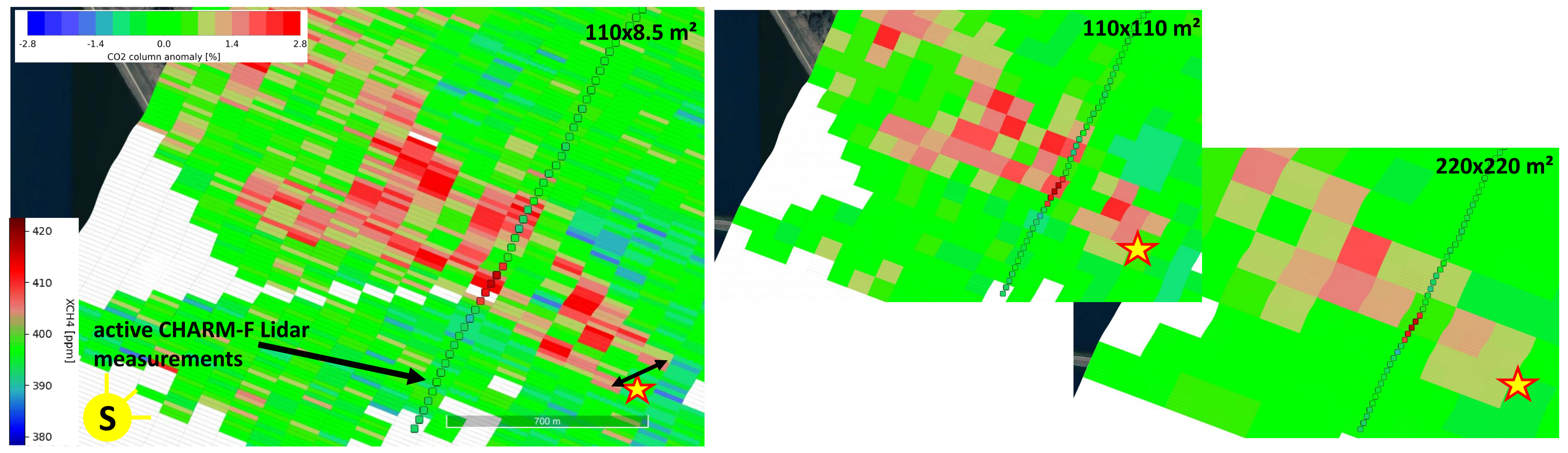

Fig. 6: CO_2 column anomalies retrieved from M2DL superimposed by absolute CO_2 columns retrieved from active CHARM-F lidar data. Left: The distance between the two starting points of the two plumes is about 170 m similar to the prediction of the simulation in *Fig. 4, bottom*. M2DL spatial resolution: about 110 m X 8.5 m. *Middle:* M2DL binned @ 110 m X 110 m. *Right:* M2DL binned @ 220 m X 220 m.

Summary & conclusions

- The '**strength**' and manifestation of **ghost plumes** is strongly dependent on **plume height in combination with vertical mixing and atmospheric stability, solar zenith angle and azimuth angle.**
- Ghost plumes are **only visible in passive remote sensing** and not in active data, as for the latter one, the plume is only vertically penetrated.
- For (typical) conditions as analyzed here (emission height: 130m, sza: 45°, perfect alignment of saa and wind direction**) plume separation is not possible** for spatial resolutions **larger than about 100 m x 100 m** according to observations & simulations.
- The appearance of ghost plumes is **usually masked by atmospheric turbulence** or **large ground scene sizes** of the instrument.
- The **results apply to both airborne and satellite-based instruments**.
- Potential impact on automated plume detection algorithms and subsequent automated processing, e.g. wind direction identification / fitting.
- Fluxes estimated from passive and active RS data should be consistent as along as the passive instrument samples both plumes. Validation will be our next step.
- Possibility of estimating mean plume height from ghost plume.

Acknowledgment:

HALO flights during CoMet 2.0 Arctic campaign have been supported by the State of Bremen, the Max Planck Society (MPG), and by the German Research Foundation (Deutsche Forschungsgemeinschaft, DFG) within the DFG Priority Program (SPP 1294) Atmospheric and Earth System Research with the Research Aircraft HALO (High Altitude and LOng Range Research Aircraft) under grant BO 1731/1-1. M2DL was built within the BMBF funded project AIRSPACE (01LK1701B)

Contact: sven.krautwurst@iup.physik.uni-bremen.de

Krautwurst, S., Fruck, C., Wolff, S., Borchardt, J., Huhs, O., Gerilowski, K., Gałkowski, M., Kiemle, C., Quatrevalet, M., Wirth, M., Mallaun, C., Burrows, J. P., Gerbig, C., Fix, A., Bösch, H., and Bovensmann, H.: Identification and Quantification of CH_4 Emissions from Madrid Landfills using Airborne Imaging Spectrometry and Greenhouse Gas Lidar, EGUsphere [preprint], https://doi.org/10.5194/egusphere-2024-3182, 2024. | **Masters**, G. M.: Introduction to Environmental Engineering and Science, Prentice-Hall, Inc., 2nd edn., 1998. | **Krings**, T., Gerilowski, K., Buchwitz, M., Reuter, M., Tretner, A., Erzinger, J., Heinze, D., Pflüger, U., Burrows, J. P., and Bovensmann, H.: MAMAP - a new spectrometer system for column-averaged methane and carbon dioxide observations from aircraft: retrieval algorithm and first inversions for point source emission rates, Atmospheric Measurement Techniques, 4, 1735–1758, doi:10.5194/amt-4-1735-2011, 2011. | **Hanna**, S. R., Briggs, G. A., and Hosker, Jr., R. P.: Handbook on Atmospheric Diffusion, 110 pp., Atmospheric Turbulence and Diffusion Laboratory, National Oceanic and Atmospheric Administration, Technical Information Center, U.S. Department of Energy, 1982. | **Borchardt**, J., Gerilowski, K., Krautwurst, S., Bovensmann, H., Thorpe, A. K., Thompson, D. R., Frankenberg, C., Miller, C. E., Duren, R. M., and Burrows, J. P.: Detection and quantification of CH_4 plumes using the WFM-DOAS retrieval on AVIRIS-NG hyperspectral data, Atmos. Meas. Tech., 14, 1267–1291, https://doi.org/10.5194/amt-14-1267-2021, 2021. | **Sánchez-García**, E., Gorroño, J., Irakulis-Loitxate, I., Varon, D. J., and Guanter, L.: Mapping methane plumes at very high spatial resolution with the WorldView-3 satellite, Atmos. Meas. Tech., 15, 1657–1674, https://doi.org/10.5194/amt-15-1657-2022, 2022.